Springer

KSME

Journal of Mechanical Science and Technology 31 (1) (2017) 429~436
www.springerlink.com/content/1738-494x(Print)/1976-3824(Online)
DOI 10.1007/s12206-016-1245-8

Mathematical modeling of torque for single screw expanders †

Yuting Wu[1,2], Ruiping Zhi[1,2,*], Wei Wang[1,2], Lili Shen[1,2], Yeqiang Zhang[3], Biao Lei[1,2], Jingfu Wang[1,2] and Chongfang Ma[1,2]

[1]*Key Laboratory of Enhanced Heat Transfer and Energy Conservation of Ministry of Education, College of Environmental and Energy Engineering, Beijing University of Technology, Beijing 100124, China*
[2]*Key Laboratory of Heat Transfer and Energy Conversion of Beijing Municipality, College of Environmental and Energy Engineering, Beijing University of Technology, Beijing 100124, China*
[3]*School of Energy and Power Engineering, Zhengzhou University of Light Industry, No.5 Dongfeng Road, Zhengzhou, Henan Province 450002, China*

(Manuscript Received April 19, 2016; Revised August 2, 2016; Accepted August 21, 2016)

Abstract

This paper presents a mathematical model of torque for Single screw expanders (SSEs). Instantaneous torque and torque ratio were analyzed and discussed. The periodic variation of instantaneous torque is the same for different inlet pressure levels. The torque ratio, with its value close to 1, is independent of the inlet pressure of SSE. An experimental system was established to measure the torque, power and shaft efficiency of the self-developed SSE prototype, and results were used to validate the model. Comparison shows that the difference between calculated and experimental torque values is small (6.58 N.m to 7.55 N.m). The calculated and experimental output power is similar, with a difference of 2.07 kW to 2.37 kW. Therefore, the proposed model can be used to estimate the torque and output power of SSEs.

Keywords: Single screw expander; Torque; Organic Rankine cycle; Waste heat recovery

1. Introduction

Organic Rankine cycle (ORC) is a promising and effective technology widely studied and used to recover low-grade waste heat [1-5]. The ORC system includes four main parts: Expander [6], pump [7], condenser and evaporator [8-10]. The expander, as a power machine, is the core and crucial to the performance of the ORC system [6].

Among many expanders such as turbine expander [11-13], scroll expander [14-18] and screw expander [19, 20-28], Single screw expander (SSE) has received considerable research attention in recent years because of its distinct advantages, such as balanced loads, long working life, simple structure, low vibration, etc. Experimental studies of ORC units based on SSE demonstrated that SSE is suitable for ORC system. SSE exhibits the maximum isentropic efficiency of 73.25 % and 64.78 %, as reported in Refs. [21, 24], respectively.

Selection of SSE is crucial to the performance of ORC systems and strongly depends on the operating conditions and magnitude of output power [6]. When an ORC system is designed for certain working conditions and the output capacity of the selected SSE is less than the heat energy recoverable from the waste heat, the system efficiency will be limited; this phenomenon may lead to erroneous selection of the motor coupling connected with the SSE. The output power of a machine can be calculated using torque. Therefore, it is a fundamental issue to establish a mathematical model of torque for SSE with given dimensions under given working operating conditions.

Previous studies on SSE mainly focused on applications and performance tests. He et al. [25] and Wang et al. [26] studied the performance of SSE with compressed air as working fluid. In Ref. [25], the measured torque of SSE considerably increases as the intake pressure increases. In Ref. [26], the shaft power exhibits a linear increasing trend with the increasing measured torque. Zhang et al. [24] tested an SSE-based ORC system for recovery of waste heat from truck engines. The performances of the ORC and SSE were investigated under different diesel working conditions and SSE torque values. It is shown that the maximum ORC efficiency was 6.48 % when the output of diesel engine was 250 kW and the torque of SSE was 64.43 N.m. Desideri et al. [21] evaluated the performance of an SSE modified from a standard compressor and developed a steady-state model of the entire ORC unit for low-capacity waste heat recovery. It is indicated that, when the rotational speed and expansion ratio were 3000 r/min and 7.7, respectively, the highest output power and isentropic efficiency

*Corresponding author. Tel.: +86 10 67391985 8323, Fax.: +86 10 67392774
E-mail address: zhiruiping@gmail.com
† Recommended by Associate Editor Tong Seop Kim

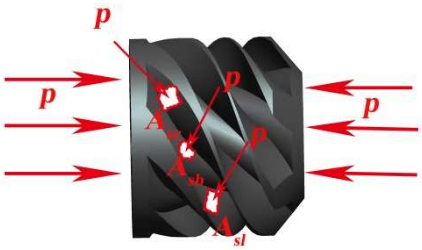

Fig. 1. Force diagram of screw rotor.

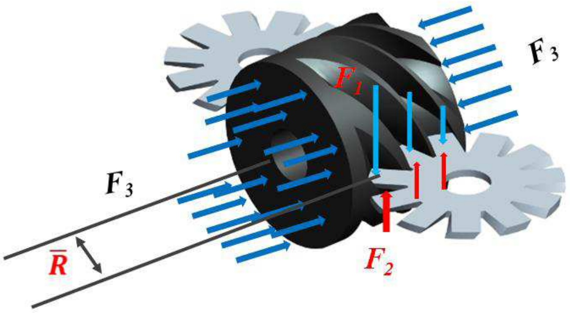

Fig. 2. Force diagram of single screw meshing pair.

were 7.8 kW and 64.7 %, respectively. In the above-mentioned experimental studies, the torque of SSEs was measured using dynamometers, but the mathematical modeling of torque for SSEs has not been investigated.

This paper aims to theoretically establish a mathematical model of torque for SSEs. The model can be used to predict instantaneous torque, torque ratio, and output power, and provides a basis for engineers to estimate the output magnitude of the SSE under given dimensions and operating conditions.

2. Mathematical modeling of torque for SSE

Two methods can be used to establish a torque mathematical model of SSE. The first method is determination of pressure, tangential projected area of the left groove surface, right groove surface and bottom surface on contact and length of the lever arm connecting the axis of screw rotor to the point of force application (Fig. 1). The mathematical model of torque is difficult to establish using this method because of the complexity of the screw groove surface. On the basis of Newton's third law, if the force on the screw rotor surface is the action force, the force on the tooth area of gate rotor is the reaction (Fig. 2). Hence, the second uses the product of the normal force F on the gate rotor meshing tooth area and centroid distance $\overline{R}$ from the centroid of the gate rotor tooth area to the center of the main rotor. Force can be calculated from pressure p and gate rotor meshing tooth area A. Furthermore, pressure at any rotational angle of gate rotor can be obtained by calculating the basic volume of SSE at any time and inlet pressure. In addition, the basic volume can be obtained using the meshing tooth area A of gate rotor and centroid distance $\overline{R}$. Therefore, in order to establish the torque model, it is of great importance to find the meshing tooth area

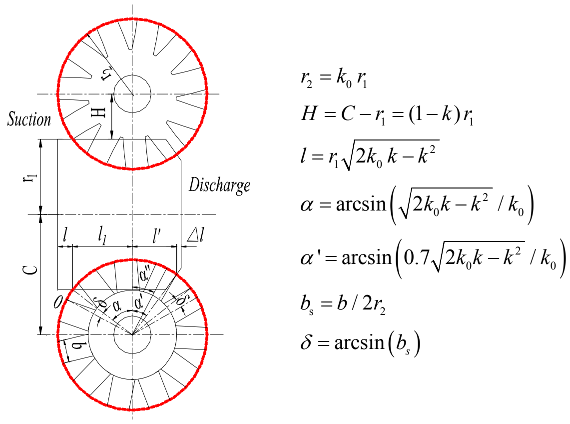

Fig. 3. Geometry relationship of meshing pair.

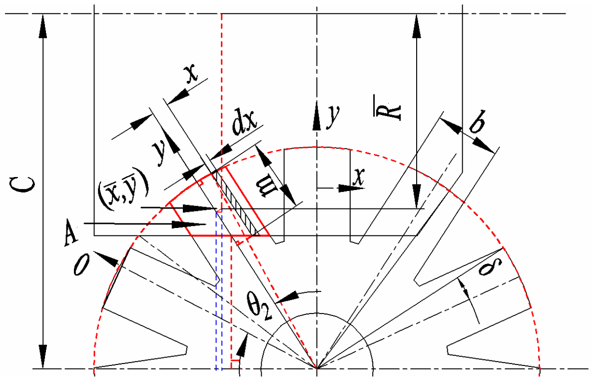

Fig. 4. Geometric analysis of meshing tooth area of gate rotor.

A of gate rotor and the centroid distance $\overline{R}$.

2.1 Geometric analysis of the single screw meshing pair

2.1.1 Meshing tooth area A of gate rotor and centroid distance

The meshing tooth area of gate rotor, as shown in Fig. 4, can be calculated by numerical integration. The relevant equation is as follows:

$$A = \begin{cases} \int_{-k_0 r_1 \sin(\theta_2 - \delta)}^{\frac{b}{2}} m dx, & 0 \le \theta_2 \le 2\delta \\ \int_{-\frac{b}{2}}^{\frac{b}{2}} m dx, & 2\delta \le \theta_2 \le \alpha + \delta + \alpha''. \end{cases} \tag{1}$$

Therefore,

$$A = \begin{cases} \int_{-k_0 r_1 \sin(\theta_2 - \delta)}^{\frac{b}{2}} \left(\sqrt{k_0^2 r_1^2 - x^2} - H\sec(\alpha + \delta - \theta_2\right) + x\tan\left(\alpha + \delta - \theta_2\right) dx, & 0 \le \theta_2 \le 2\delta \\ \int_{-\frac{b}{2}}^{\frac{b}{2}} (\sqrt{k_0^2 r_1^2 - x^2} - H\sec(\alpha + \delta - \theta_2) + x\tan\left(\alpha + \delta - \theta_2\right) dx, & 2\delta \le \theta_2 \le \alpha + \delta + \alpha''. \end{cases} \tag{2}$$

The distance $\overline{R}$ can be obtained by finding the centroid $(\overline{x}, \overline{y})$ of meshing tooth area of gate rotor and the center distance C. The centroid $(\overline{x}, \overline{y})$ and the distance $\overline{R}$ can be expressed as:

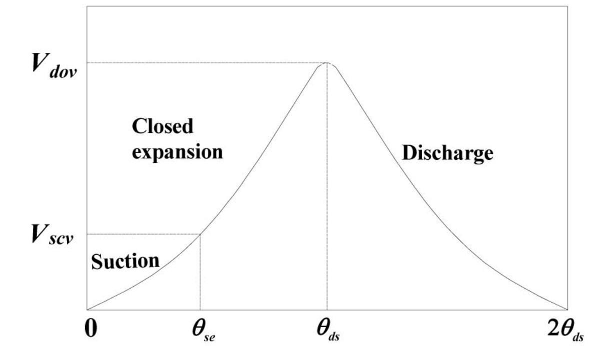

Fig. 5. Simplified working process diagram of SSEs.

When $0 \le \theta_2 \le 2\delta$,

$$\begin{cases} \overline{x} = \int_{-k_0 r_1 \sin(\theta_2 - \delta)}^{\frac{b}{2}} mxdx / A \\ \overline{y} = \int_{-k_0 r_1 \sin(\theta_2 - \delta)}^{\frac{b}{2}} m(\sqrt{k_0^2 r_1^2 - x^2} - \frac{m}{2})dx / A \\ \overline{R} = C - \overline{x}\sin(\alpha + \delta - \theta_2) - \overline{y}\cos(\alpha + \delta - \theta_2) . \end{cases} \tag{3}$$

When $2\delta \le \theta_2 \le \alpha + \delta + \alpha''$,

$$\begin{cases} \overline{x} = \int_{-\frac{b}{2}}^{\frac{b}{2}} mxdx / A \\ \overline{y} = \int_{-\frac{b}{2}}^{\frac{b}{2}} m(\sqrt{k_0^2 r_1^2 - x^2} - \frac{m}{2})dx / A \\ \overline{R} = C - \overline{x}\sin(\alpha + \delta - \theta_2) - \overline{y}\cos(\alpha + \delta - \theta_2) . \end{cases} \tag{4}$$

2.1.2 Basic volume of screw rotor

As illustrated in Fig. 5, the entire expansion process in SSE can be divided into three phases: Suction, closed expansion and discharge. The first part of volume is an inherent suction volume for each main rotor when the angle of the gate rotor is between 0 and 2δ . The suction volume of SSE at any time during the suction phase can be given as follows:

$$V_{sbv} = \int_0^{2\delta} Ai\overline{R}d\theta_2 + \int_{2\delta}^{\theta_2} Ai\overline{R}d\theta_2,\ 2\delta \le \theta_2 \le \theta_{se} \ . \tag{5}$$

The closed expansion volume at any time during the closed expansion phase can be written as follows:

$$V_{cbv} = \int_0^{2\delta} Ai\overline{R}d\theta_2 + \int_{2\delta}^{\theta_2} Ai\overline{R}d\theta_2,\ \theta_{se} \le \theta_2 \le \theta_{ds} \ . \tag{6}$$

The discharge volume at any time during the discharge phase can be calculated as:

$$V_{ds} = \begin{cases} \int_0^{2\delta} Ai\overline{R}d\theta_2 + \int_{2\delta}^{\theta_2} Ai\overline{R}d\theta_2,\ \theta_{ds} \le \theta_2 \le 2\theta_{ds} - 2\delta \\ \int_0^{2\delta} Ai\overline{R}d\theta_2,\ 2\theta_{ds} - 2\delta \le \theta_2 \le 2\theta_{ds} \ . \end{cases} \tag{7}$$

2.2 Mathematical modeling of torque

Assuming that the pressure on the lower teeth surface of gate rotor is equal to the discharge pressure, the instantaneous torque is divided into three phases according to the operation of SSE. Assuming that the process is reversible process during the closed expansion, the instantaneous torque for one tooth of gate rotor can be expressed as follows:

$$T = (F_1 - F_2)\overline{R} = \begin{cases} \left(p_{in} - p_{out}\right)A\overline{R}, 0 \le \theta_2 \le 2\delta \\ \left(p_{in} - p_{out}\right)A\overline{R}, 2\delta < \theta_2 \le \theta_{se} \\ \left(p\left(V_{ce}, s_{in}\right) - p_{out}\right)A\overline{R},\ \theta_{se} < \theta_2 \le \theta_{ds} \\ \left(p_{out} - p_{out}\right)A\overline{R}, \theta_{ds} < \theta_2 \le 2\theta_{ds} \ . \end{cases} \tag{8}$$

Inlet pressure losses are not considered, because there is no inlet valve for single screw expander and the inlet port is large. Moreover, the discharge pressure p_{out} and $p(V_{ce}, s_{in})$ are derived after considering the leakage losses and can be estimated by the formulae given by Shen et al. [28].

The gate rotor teeth are circumferentially equispaced; thus, the angel between adjacent two teeth is $\gamma = 360 / z_2$. When the screw rotor meshes with a pair of gate rotors which is symmetrical along the axis, almost two or three meshed teeth for one gate rotor are present. Therefore, the instantaneous torque in SSE can be established as:

$$T_S = T\left(\theta_2\right) + T\left(\theta_2 + \gamma\right) + T\left(\theta_2 + 2\gamma\right) . \tag{9}$$

Consequently, the average torque is given as follows:

$$\overline{T} = \frac{\int_{t_1}^{t_2} T_S\, dt}{t_2 - t_1} . \tag{10}$$

The shaft efficiency can be divided into the product of the leakage efficiency η_{le}, the internal flow efficiency η_{in} and the mechanical efficiency η_{me}. The leakage losses have been considered in the above pressure calculation, so the following calculated torque only needs to consider the internal flow efficiency η_{in} and the mechanical efficiency η_{me}. The calculated torque can be obtained as:

$$\overline{T}_{ca} = \eta_{in}\,\eta_{me}\,\overline{T} \ . \tag{11}$$

According to the experimental data in Table 2, the shaft efficiency is set to 50 % in theoretical calculation. According to the empirical volumetric efficiency, the leakage efficiency is assumed as 80 %. Thus, based on the above empirical data, $\eta_{in}\,\eta_{me}$ is set to 62.5 % in the following calculation.

The calculated output can be described as:

$$P_{cop} = \frac{\overline{T}_{ca}\, n}{9550} . \tag{12}$$

Torque ratio is defined as the theoretical torque at different angles of screw rotor to the average torque of SSE, which can reflect whether SSE runs smoothly or not. If the torque ratio is close to 1, it indicates that the SSE runs relatively smoothly. The torque ratio can be calculated as:

$$\lambda = \frac{T_S}{\bar{T}} . \tag{13}$$

3. Experimental study

3.1 Test bench description

An experimental study on an SSE prototype with 155 mm diameter screw rotor was carried out on a self-made compressed-air-based test bench; the general layout is given in Fig. 6. As described in the Fig. 6, this experimental system consists of five parts: air intake and exhaust circuit, oil lubrication circuit, power testing system, water cooling system, and data acquisition system. The SSE prototype was specifically designed by our laboratory, and thus it is not originally a single screw compressor in reverse. It drives an electric eddy current dynamometer, which is used to measure the torque and output power of SSE. The air source is a compressed air storage tank with high-capacity. The air pressure flowing into the expander can be controlled by adjusting the governor valve. The dynamometer is cooled with water. A water pump drives water from cooling tower to the dynamometer exhaust. The experimental platform is shown in Fig. 7, and the key parameters of SSE are listed in Table 1.

Table 1. SSE key parameters.

Parameters	
Diameter of main rotor	155 mm
Diameter of gate rotor	155 mm
Transmission ratio	11/6
Center distance	124 mm
Volume ratio	5
Tooth width of gate rotor	23.4 mm

3.2 Achieved performance

Performance analyses were carried out by varying the intake pressure p_{in} from 4.971 to 9.975 bar and maintaining the speed at 2999~3000 rpm. The expander shaft power and shaft efficiency are taken into account. The experimental results are given in Table 2.

4. Results and validation

Based on the established torque model, relevant Matlab codes are programmed and developed to obtain the pressure,

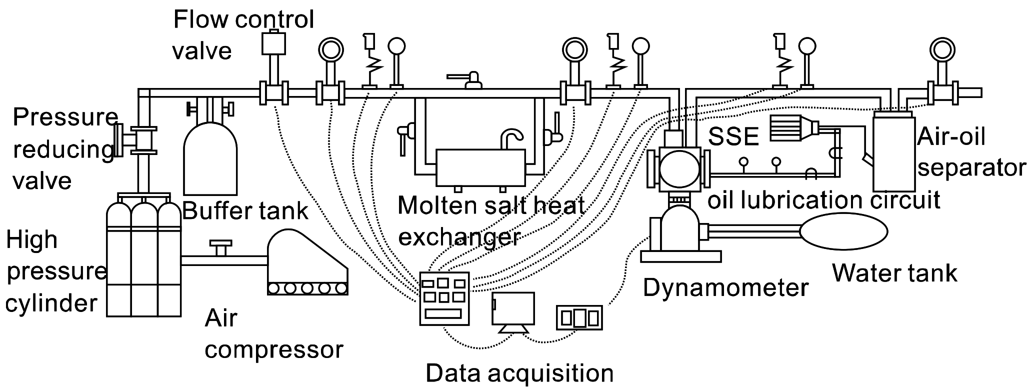

Fig. 6. General layout of the test bench.

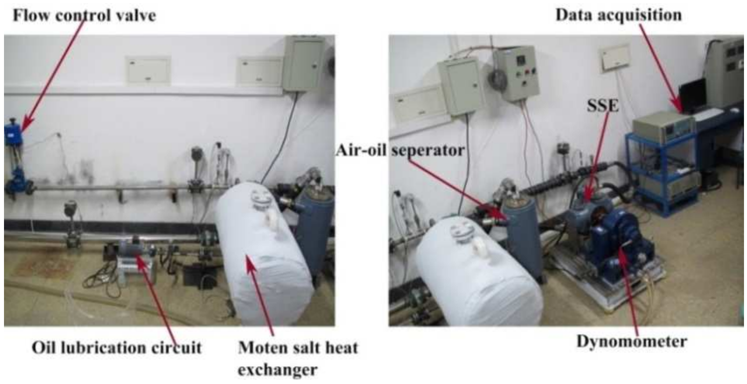

Fig. 7. Test bench platform.

Table 2. Experimental results of SSE.

Inlet pressure, p_{in} (bar)	Rotate speed, n (r/min)	Torque, T_{ex} (N.m)	Output power, P_{ex} (kW)	Outlet pressure, p_{ds} (bar)	External expansion ratio, ε_d	Shaft efficiency, η_s (%)
4.971	2999	11.464	3.600	0.500	3.981	48.189
5.976	3000	15.785	4.958	0.600	4.340	51.387
7.033	2999	20.166	6.333	0.700	4.725	54.046
8.010	2999	24.028	7.457	0.800	5.005	56.393
8.975	3000	27.776	8.72	0.967	5.073	57.679
9.975	3000	31.583	9.92	1.100	5.226	58.274

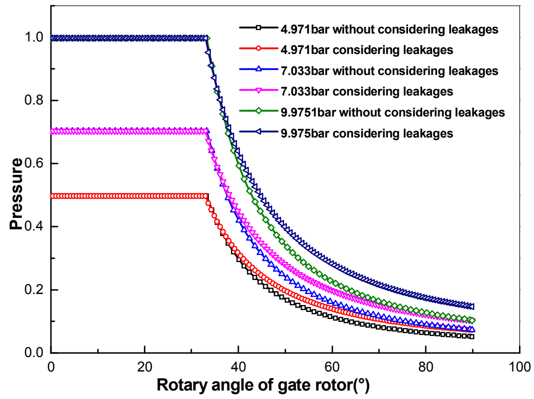

Fig. 8. Pressure versus rotary angle of gate rotor.

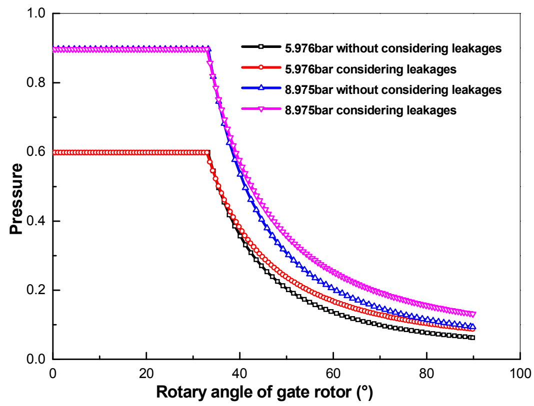

Fig. 9. Pressure versus rotary angle of gate rotor.

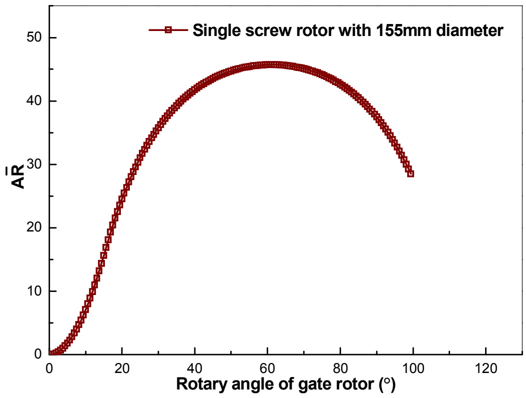

Fig. 10. Product value of $A\bar{R}$ versus rotary angle of gate rotor.

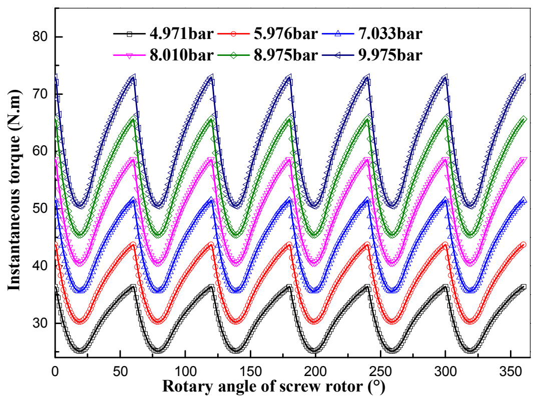

Fig. 11. Instantaneous torque of SSE versus rotary angle of screw rotor.

product of meshing tooth area A and centroid distance $\bar{R}$, instantaneous torque of SSE and toque ratio with the rotational angle changes of screw rotor, the average torque, the calculated torque and the output power. The inlet pressure is assumed equal to the values measured in experiments, and expansion process is a perfect adiabatic expansion.

In Figs. 8 and 9, it is shown that the pressure value after considering leakages is higher than that without considering leakages during closing expansion and discharge starting phase. It indicates that the leakage losses lead to increase in discharge pressure. Fig. 10 describes the product value of meshing tooth area of gate rotor A and centroid distance $\bar{R}$ when a tooth of the gate rotor meshes with a single groove of the screw rotor used in experimental system and shows that the product value first increases and then decreases with rotary angle of gate rotor.

It can be seen from Fig. 11 that the instantaneous torque varies with a period of 60°. In a period, all the relative highest and lowest points occur at the same degrees, despite varied levels of inlet pressure. The output torque of SSE increases with the growth of inlet pressure. This trend is consistent with that of the experimental results.

The torque ratio is close to 1, which indicates that the SSE runs smoothly. As observed in Fig. 12, the torque ratio is independent of the inlet pressure, and there is a small fluctuation (between -0.2 and +0.2) of torque ratio around the horizontal line (the torque ratio at the horizontal line is equal to 1). Therefore, the SSE runs steadily.

On the basis of the trapezoid rule of numerical integral formulas, the average torque in one period can be obtained using

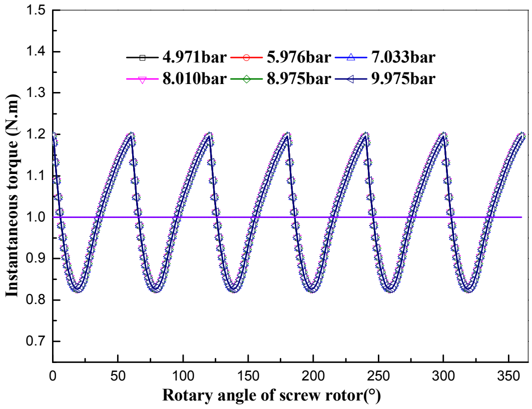

Fig. 12. Torque ratio of SSE versus rotary angle of screw rotor.

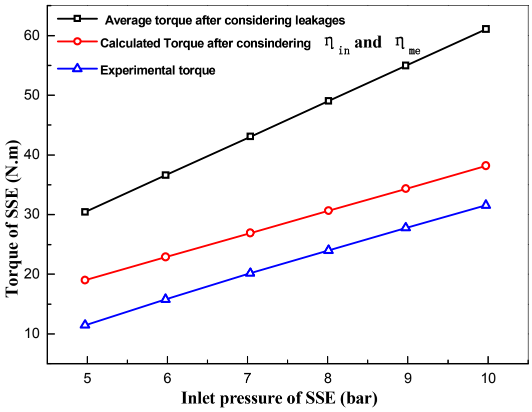

Fig. 13. Torque of SSE versus inlet pressure.

Eq. (10). In Fig. 13, the average, calculated and experimental torque shows a linear increasing trend with increasing inlet pressure. Hence, torque is proportional to the inlet pressure of SSE. Furthermore it can be seen that the average torque is greater by 19 N.m than the experimental torque because the mechanical and internal flow losses are not considered. After considering the mechanical and internal flow efficiency, the calculated torque is slightly greater than the experimental torque. The difference between calculated torque and experimental torques is small (6.58 N.m~7.55 N.m). Thus the torque can be estimated using the proposed model.

In the Fig. 14, the calculated output power and experimental output power of SSE increase linearly with the growth of inlet pressure. It is shown that the calculated output power is much closer to the experimental one, and that the difference value (ΔP_{cop}) in the output power ranges from 2.07 to 2.37 kW. Therefore, there is a minor difference value between calculated output power and experimental output power. Thus, to some extent, the calculated output power can be used to estimate the output power of SSEs.

5. Conclusions

The intention of this paper is to present a mathematical model of torque for SSE, which is a promising power machine

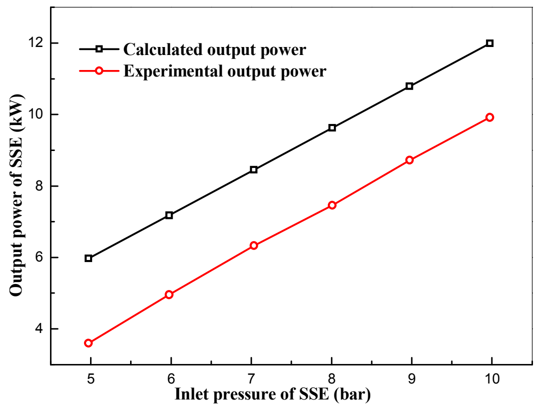

Fig. 14. Output power of SSE versus inlet pressure.

in ORC and refrigeration systems. Experimental studies on SSE by using compressed air as working fluid were carried out to validate the proposed torque model. The following conclusions can be drawn:

(1) The periodic change in instantaneous torque with changes in rotational angle of screw rotor is the same under different pressure levels. The instantaneous torque increases with the rise of inlet pressure, consistent with the test results. The torque ratio remains constant despite variations in the inlet pressure of SSE, indicating that the SSE runs steadily.

(2) Comparison between predicted values and experimental results shows a fairly good agreement, particularly when the mechanical losses, internal flow losses and leakages are taken into account. Hence, the proposed torque model can be used to estimate the torque and output power of SSEs under given dimensions and operating conditions.

Acknowledgements

This work was sponsored by the National Basic Research Program of China (Grant Number 2013CB228306) and the International Science and Technology Cooperation Program of China (Grant Number 2014DF60600).

Nomenclature

i : Transmission ratio (−)
θ_1 : Rotary angle of screw rotor (rad)
θ_2 : Rotary angle of gate rotor (rad)
z_2 : Number of gate rotor teeth (−)
γ : Indexing angle of gate rotor (rad)
k_0 : Ratio of the main rotor radius in to the gate rotor radius (−)
k : Meshing depth coefficient (−)
r_1 : Radius of screw rotor (mm)
r_2 : Radius of gate rotor (mm)
H : The distance from center of gate rotor to outer side of screw rotor (mm)
C : Center distance of single screw meshing pair (mm)
l : Axial length of the discharge side (mm)

α : Meshing angle of the discharge side (rad)
α' : Meshing angle of the suction side (rad)
α'' : Key angle deciding the discharge starting angle (rad)
l' : Axial length of the suction side (mm)
ξ : Coefficient of the groove wall (−)
e : Minimum width of the groove wall (mm)
b : Tooth width of the gate rotor (mm)
b_s : Tooth width coefficient (−)
δ : Half angle of the tooth width (rad)
A : Area of gate rotor tooth meshing with main rotor (mm^2)
T_s : Instantaneous torque of SSE (N.m)
$\overline{R}$: Centroid distance from centroid of the gate rotor tooth area to the center of screw rotor (mm)
p_{in} : Inlet pressure of SSE (Mpa)
p_{out} : Outlet pressure of SSE (Mpa)
V_{ce} : Basic volume during closing expansion (Mpa)
θ_{se} : Suction ending angle (rad)
θ_{ds} : Discharge starting angle (rad)
$\overline{T}$: Average torque (N.m)
$\overline{T}_{ca}$: Calculated torque after considering the efficiency (N.m)
η_{le} : Leakage efficiency (%)
η_{in} : Internal flow efficiency (%)
η_{me} : Mechanical efficiency (%)
η_s : Shaft efficiency (%)
λ : Torque ratio (−)
p_{cop} : Calculated output power (kW)
n : Rotational speed of SSE (r/min)
s_{in} : Inlet entropy of SSE (kJ/kg.K)

References

[1] C. Sprouse and C. Depcik, Review of organic Rankine cycles for internal combustion engine exhaust waste heat recovery, *Applied Thermal Engineering*, 51 (1-2) (2013) 711-722.

[2] M. Imran, B. S. Park, H. J. Kim, D. H. Lee and M. Usman, Economic assessment of greenhouse gas reduction through low-grade waste heat recovery using organic Rankine cycle (ORC), *Journal of Mechanical Science and Technology*, 29 (2) (2015) 835-843.

[3] E. Yun, H. Park, Y. Y. Sang and K. C. Kim, Dual parallel organic Rankine cycle (ORC) system for high efficiency waste heat recovery in marine application, *Journal of Mechanical Science and Technology*, 29 (6) (2015) 2509-2515.

[4] E. H. Wang, H. G. Zhang, B. Y. Fan and Y. T. Wu, Optimized performances comparison of organic Rankine cycles for low grade waste heat recovery, *Journal of Mechanical Science and Technology*, 26 (8) (2012) 2301-2312.

[5] X. W. Gong, X. Q. Wang, Y. R. Li and C. M. Wu, Thermodynamic performance analysis of a coupled transcritical and subcritical organic Rankine cycle system for waste heat recovery, *Journal of Mechanical Science and Technology*, 29 (7) (2015) 3017-3029.

[6] G. Q. Qiu, H. Liu and S. Riffat, Expanders for micro-CHP systems with organic Rankine cycle, *Applied Thermal Engineering*, 31 (16) (2011) 3301-3307.

[7] Y. T. Wu, B. Lei, C. F. Ma, L. Zhao, J. F. Wang, H. Guo and Y. W. Lu, Study on the characteristics of expander power output used for offsetting pumping work consumption in organic Rankine cycles, *Energies*, 7 (2014) 4957-4971.

[8] X. L. Luo, Z. T. Yi, Z. W. Chen, Y. Chen and S. P. Mo, Performance comparison of the liquid-vapor separation, parallel flow, and serpentine condensers in the organic Rankine cycle, *Applied Thermal Engineering*, 94 (2016) 435-448.

[9] S. Y. Wu, C. Li, L. Xiao, Y. R. Li and C. Liu, The role of outlet temperature of flue gas in organic Rankine cycle considering low temperature corrosion, *Journal of Mechanical Science and Technology*, 28 (12) (2014) 5213-5219.

[10] J. J. Xu, X. L. Luo, Y.Chen and S. P. Mo, Multi-criteria design optimization and screening of heat exchangers for a subcritical ORC, *Energy Procedia,* 75 (2015) 1639-1645.

[11] R. Capata and G. Hernandez, Preliminary design and simulation of a turbo expander for small rated power organic Rankine cycle (ORC), *Energies*, 7 (11) (2014) 7067-7093.

[12] Y. P. Xie, Prospect of application and development of Low saturation steam turbine, *Energy Conservation Technology* (2011).

[13] S. Han, J. B. Seo and B.-S. Choi, Development of a 200 kW ORC radial turbine for waste heat recovery, *Journal of Mechanical Science and Technology*, 28 (12) (2014) 5231-5241.

[14] S. Quoilin, V. Lemort and J. Lebrun, Experimental study and modeling of an organic Rankine cycle using scroll expander, *Applied Energy*, 87 (4) (2010) 1260-1268.

[15] J. C. Chang, T. C. Hung, Y. L. He and W. P. Zhang, Experimental study on low-temperature organic Rankine cycle utilizing scroll type expander, *Applied Energy*, 155 (2015) 150-159.

[16] V. Lemort, S. Quoilin, C. Cuevas and J. Lebrun, Testing and modeling a scroll expander integrated into an Organic Rankine Cycle, *Applied Thermal Engineering*, 29 (14) (2009) 3094-3102.

[17] V. Lemort, S. Declaye and S. Quoilin, Experimental characterization of a hermetic scroll expander for use in a micro-scale Rankine cycle, *Proceedings of the Institution of Mechanical Engineers Part A Journal of Power and Energy*, 226 (1) (2011) 126-136.

[18] H. Wang, R. B. Peterson and T. Herron, Experimental performance of a compliant scroll expander for an organic Rankine cycle, *Proceedings of the Institution of Mechanical Engineers Part A Journal of Power and Energy*, 223 (7) (2009) 863-872.

[19] H. Leibowitz, I. K. Smith and N. Stosic, Cost effective small scale orc systems for power recovery from low grade heat sources, *ASME 2006 International Mechanical Engineering Congress and Exposition*, 53 (7) (2006) 521-527.

[20] Y. Q. Zhang, Y. T. Wu, W. He, G. D. Xia, C. F. Ma and Y. H. Peng, Experimental study on the influence of rotational

speed on the performance of a single-screw expander with a 175 mm screw diameter, *International Journal of Green Energy*, 12 (3) (2015) 257-264.
[21] A. Desideri, M. van den Broek, S. Gusev, V. Lemort and S. Quoilin, Experimental campaign and modeling of a low-capacity waste heat recovery system based on a single screw expander, *Proceedings of 22nd International Compressor Engineering Conference,* Purdue (2014) 1451.
[22] Y. W. Lu, W. He, Y. T. Wu, C. F. Ma and H. Guo, Performance study on compressed air refrigeration system based on single screw expander, *Energy*, 55 (2013) 762-768.
[23] W. Wang, Y. T. Wu, C. F. Ma, G. D. Xia and J. F. Wang, Experimental study on the performance of single screw expanders by gap adjustment, *Energy*, 62 (2013) 379-384.
[24] Y. Q. Zhang, Y. T. Wu, G. D. Xia, C. F. Ma, W. N. Ji, S. W. Liu, K. Yang and F. B. Yang, Development and experimental study on organic Rankine cycle system with single-screw expander for waste heat recovery from exhaust of diesel engine, *Energy*, 77 (2014) 499-508.
[25] W. He, Y. T. Wu, Y. H. Peng, Y. Q. Zhang, C. F. Ma and G. Y. Ma, Influence of intake pressure on the performance of single screw expander working with compressed air, *Applied Thermal Engineering*, 51 (1) (2013) 662-669.
[26] W. Wang, Y. T. Wu, C. F. Ma, L. D. Liu and J. Yu, Preliminary experimental study of single screw expander prototype, *Applied Thermal Engineering*, 31 (17) (2011) 3684-3688.
[27] G. S. Sun, The investigation of some basic geometric problems of the single screw compressor, *International Compressor Engineering Conference* (1988) 630.
[28] L. L. Shen, W. Wang and Y. T. WU, Theoretical analysis of variation of leakage path length in single screw expander, *Journal of Mechanical Engineering* (2015).

Yuting Wu got his doctorate from Beihang University, China, in 2000. From 2000 to 2002, he worked in Tsinghua University as a post doctor. Later he taught at Beijing University of Technology. Now he is a Researcher of the College of Environmental and Energy Engineering. His research interests include organic Rankine cycle technology recovering low-grade heat, solar thermal power, advanced refrigeration technology and molten salt for heat storage.

Ruiping Zhi got her master's degree from China University of Petroleum, China, in 2012. Now she is a post-graduate student at Beijing University of Technology. Her research interests include key components of single screw compressor and expander and organic Rankine cycle for waste heat recovery.